

Acoustic Leak Detection in Water Networks

Robert Müller¹^a, Steffen Illium¹^b, Fabian Ritz¹^c, Tobias Schröder², Christian Platschek²,
Jörg Ochs² and Claudia Linnhoff-Popien¹^d

¹Mobile and Distributed Systems Group, LMU Munich, Germany
{robert.mueller, steffen.illum, fabian.ritz, linnhoff}@ifi.lmu.de

²Stadtwerke München GmbH, Germany
{schroeder.tobias, platschek.christian, ochs.joerg}@swm-infrastruktur.de

Keywords: Leak Detection, Water Networks, Acoustic Anomaly Detection, Applied Machine Learning

Abstract: In this work, we present a general procedure for acoustic leak detection in water networks that satisfies multiple real-world constraints such as energy efficiency and ease of deployment. Based on recordings from seven contact microphones attached to the water supply network of a municipal suburb, we trained several shallow and deep anomaly detection models. Inspired by how human experts detect leaks using electronic sounding-sticks, we use these models to repeatedly listen for leaks over a predefined decision horizon. This way we avoid constant monitoring of the system. While we found the detection of leaks in close proximity to be a trivial task for almost all models, neural network based approaches achieve better results at the detection of distant leaks.

1 Introduction

Leakage is one of the main causes for water loss in water supply and distribution networks. Undetected leaks, which usually occur due to corrosion and soil movement, may have extensive negative effects on the surrounding infrastructure, customer convenience and financial profit. Contributing to this problem is the fact that it can take a considerable amount of time until a leak is detected, localized and countermeasures are put into place.

In the UK, approximately 3200 Million liters of water are wasted due to leakages in water networks every day (WaterUK, 2020), a disproportionately high value with regard to climate change and a shortage of drinking water in many countries. Greater efforts are needed to minimize water loss through leakages.

A reliable indicator for substantial water loss is the deviation of the zero-consumption status in a balance area at night. But if a leakage is more subtle, it is usually not detected until water emerges from the surfaces and residents report the issue.

Locating the source by means of the acoustic emis-

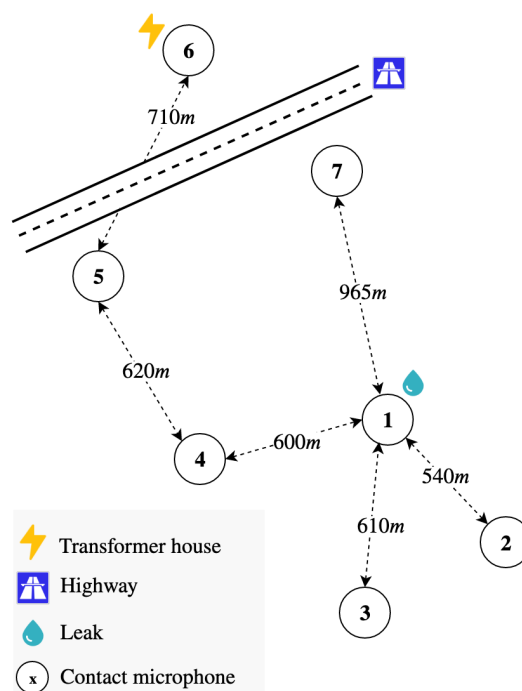






Figure 1: Simplified map of the location of each contact microphone and significant objects in their neighborhood. For each contact microphone, we depict the distance of the shortest pipeline link to another contact microphone. Note that distance is given in meters of water pipe.

^a <https://orcid.org/0000-0003-3108-713X>

^b <https://orcid.org/0000-0003-0021-436X>

^c <https://orcid.org/0000-0001-7707-1358>

^d <https://orcid.org/0000-0001-6284-9286>

sion from exiting water is one the predominantly used approaches (El-Zahab and Zayed, 2019). The process is as follows:

1) *Leak noise correlation*: Liquid escaping a pipe creates shock waves that cause the pipe to vibrate, resulting in a characteristic leak sound. At least two sensors are attached to the pipe around the presumed leak location. By analyzing the variation in propagation times of the leak’s acoustic emission between the sensors, the location is further narrowed down. This approach requires infrastructural knowledge, such as pipe material, diameter, length and corresponding sound velocities.

2) *Electro-acoustic method*: To further pinpoint the location, human leak detection experts search for leak noises using electronic sounding sticks. A leak can be localized by exploiting the fact that leak sounds become more dominant as the expert approaches the leak. The process relies on trained human experts and requires a solid estimate of the leakage location as finding the first evidence might otherwise become very time consuming.

In this work, we aim to automatize the electro-acoustic method utilizing machine learning. We record normal operation data using seven contact microphones attached on various parts of the water supply network in a suburban area of Munich. Subsequently, we train several unsupervised anomaly detection models and embed these into a broader procedure that satisfies several real world constraints, such as energy consumption and limited bandwidth. Our approach can be understood as a first step towards a fully automatized leak detection system that does not need to wait for leak aftereffects to appear. Moreover, our approach is data-driven and does not require a detailed mathematical model of the water network’s inner workings.

The rest of the paper is structured as follows: In Section 2 we briefly review related work. Then we motivate and propose a general procedure for acoustic leak detection in Section 5. In Section 4 we describe the data acquisition process followed by the description of the experimental setup and its evaluation. We close by summarizing our findings in Section 6 and laying out future work in Section 7

2 Related Work

Related approaches of acoustic leak detection are mostly based on cross-correlation (Muggleton and Brennan, 2004; Gao et al., 2017), wavelet transforms (Ni and Iwamoto, 2002; Ting et al., 2019), Support-Vector-Machines (Kang et al., 2017; Cody

et al., 2017) or neural networks (Kang et al., 2017; Chuang et al., 2019; Cody et al., 2020). Other methods combine acoustic data with additional sensory measurements (Stoianov et al., 2007). Their performance depends on the pipe network material (e.g. polyethylene or metal). However, none of these approaches directly matches the setup and constraints of this work as experiments are mostly carried out under laboratory conditions and only study a single algorithmic approach. Other physical phenomena that occur in presence of a leak can also be taken advantage of, e.g. using thermography, ground penetration radar or pressure-based methods. An exhaustive summary can be found in (Adedeji et al., 2017; Chan et al., 2018). Apart from leak detection, the broader field of acoustic anomaly detection has recently gained traction. Most of the recent work in the field is based upon Deep-Autoencoders (AEs). An AE learns to reconstruct its input from a compressed latent representation. Unseen, anomalous data is assumed to have a higher reconstruction error. The approaches mostly differ in the architecture used.

Duman et al. (Duman et al., 2019) use a deep convolutional AE on the spectrograms of sounds from industrial processes. In (Meire and Karsmakers, 2019) the authors also conclude that convolutional AEs perform well on the task of acoustic anomaly detection while they have also found the One-Class Support Vector Machine to be a strong competitor. In the same vein, Müller et al. (Müller et al., 2020) use pretrained convolutional neural networks for feature extraction and train various traditional anomaly detection models. Other work (Marchi et al., 2015; Li et al., 2018; Nguyen et al., 2019) explicitly takes the sequential nature of sound into account by training a recurrent AE based on Long-Short-Term Memory. Koizumi et al (Koizumi et al., 2017) use a more traditional Feed-Forward AE in conjunction with a novel loss function based on statistical hypothesis testing. This approach requires the simulation of anomalous sounds by using rejection sampling. Recently, Suefusa et al. (Suefusa et al., 2020) proposed to alter the input an AE receives to improve the detection of non-stationary sounds. Instead of predicting all spectrogram frames, they remove the center frame and use it as prediction target thereby alleviating the difficulty of predicting the edge frames.

Another line of work investigates upon methods that operate directly on the raw waveform (Hayashi et al., 2018; Rushe and Namee, 2019). WaveNet-like (Oord et al., 2016) generative architectures that utilize causal-dilated convolutions are used to predict the next sample. The prediction error serves as the anomaly score.

3 Motivation and Problem Definition

An automated leak detection system should be energy efficient, easy to deploy and easy to update. We derive the problem definition from the following deployment scenario: Small battery driven IoT devices record sounds from contact microphones upon request from a central control unit. During a predefined period, sounds are periodically recorded for a short time frame (2-5s). Afterwards, the collection of short audio sequences is transmitted to the central control unit via a low energy, low bandwidth radio network (SWM, 2018). This reduces the high energy and bandwidth consumption that constant monitoring would cause. The central control unit can then put all received measurements in context to decide whether a leak is present or not. Moreover, using a central control unit makes updating the system (e.g. changing the algorithm or retraining the model) more feasible. This approach is inspired by how human leak detection experts make decisions using electronic sounding sticks. After attaching the stick on to a hydrant connection, the expert listens carefully for up to ten seconds. When facing audible noise emitted by infrastructure, agriculture or industry, the process is repeated until an accurate decision can be made. For precise leak localization, various hydrant or valve connections in the area are checked accordingly. Increasing leak sounds indicate a decreased distance to the leak. In this work, we focus on leak detection and leave localization for future work. Our approach is formulated as follows:

Problem Definition 1. Let X be some representation of an h minute recording from a contact microphone on a water pipe. Further, let $\mathcal{F}_\theta : Y \rightarrow \mathbb{R}_+$ be some trainable function with parameters θ where Y is a sample of X with a length of t seconds. Apply \mathcal{F}_θ on m different sections of X to obtain a vector $\in \mathbb{R}_+^m$ of positive real valued anomaly scores. To compute a single anomaly score for X , combine the measurements using an aggregation function $\phi : \mathbb{R}_+^m \rightarrow \mathbb{R}_+$. Find $(\mathcal{F}_\theta, \phi, h, t, m)$ such that the anomaly scores for leak sections are higher than the anomaly-scores for no-leak sections.

The accompanying algorithm is depicted in Algorithm 1. Note that the sampling timepoints are equally distributed across the whole recording (Line 3), i.e. `linspace` returns the set

$$\left\{ \left\lfloor i * \frac{(h-t)}{m} \right\rfloor \mid i \in 1, \dots, m \right\}$$

and each sample is preprocessed (Line 7) to fit the domain of the score function (e.g. spectrum, raw-audio

Algorithm 1: Acoustic Leak Detection

Input: Audio recording X

Parameters: Score func. \mathcal{F}_θ , Aggregation func. ϕ , Number of samples m , Sample length t , preprocessing func. ρ

Output: Anomaly Score for X

```

1 begin
2    $h \leftarrow \text{length}(X)$ 
3    $P \leftarrow \text{linspace}(0, h-t, m)$ 
4    $S \leftarrow []$ 
5   for  $p$  in  $P$  do
6      $x \leftarrow X[p : p+t]$ 
7      $\tilde{x} \leftarrow \rho(x)$ 
8      $s \leftarrow \mathcal{F}_\theta(\tilde{x})$ 
9     append  $s$  to  $S$ 
10  end
11  return  $\phi(S)$ 
12 end
```

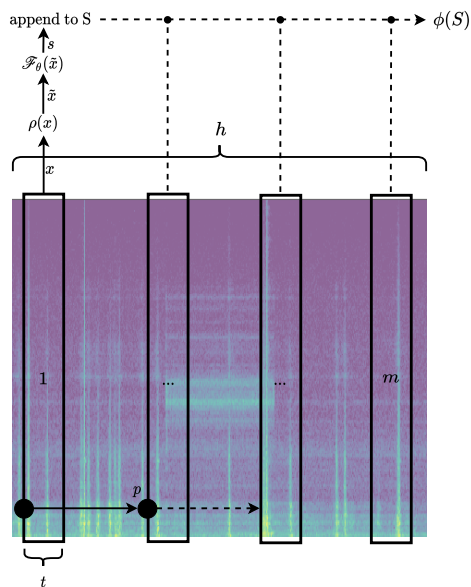


Figure 2: Visualization of the most important aspects of our acoustic leak detection approach.

or feature vector). We also depict the most important aspects of the method visually in Figure 2. To obtain enough leak sound recordings for supervised learning, one would have to artificially create a vast amount of leaks. Furthermore, for these recordings to contain enough diversity, this would have to be done on various sections of the water network. Due to the financial and environmental issues that would arise, we assume that \mathcal{F}_θ is trained on normal operation data only.

4 Data Acquisition

For data acquisition, a suburban part of Munich with little traffic was chosen as a testing ground. Seven contact microphones were directly attached onto hydrants of an iron pipe network (\varnothing 100mm). Figure 1 shows a simplified map marking the locations of the microphones as well as significant objects in the surrounding area that might influence the quality of the recordings. Sounds were recorded for three months. To avoid excessively high signals (overdrive), we kept the pre-amplifier, equalizer and post-amplifier neutral, effectively recording sounds "as-is" and disabling the dynamic sensitivity adjustment. This leads to the recordings having a headroom of 24 dB on average. All contact microphones are designed to record sounds reliably between 300Hz and 3000Hz. During the time of recording, a medium sized water leakage occurred in close proximity (\approx 20m) to contact microphone one (see Figure 1). The leak was present for 28 days and was fixed thereafter. Furthermore, we conducted various field tests. We simulated a leakage by opening a hydrant near contact microphone five and attached a contact microphone to hydrant connections between contact microphone four and five every 100 meters. Overall, we were neither able to hear the leak nor able to observe typical leak patterns in the frequency spectrograms beyond a distance of 600 meters.

5 Evaluation

In this section, we conduct various experiments to find an appropriate setting of $(\mathcal{F}_\theta, \phi, h, t, m)$. First we introduce the dataset followed by a brief discussion of the anomaly detection models that were used. Finally, we present the experiments and results.

5.1 Methodology and Dataset

The evaluation set up is designed to line up with Problem Definition 1. We use 600 hours of normal operation recordings equally sampled from all contact microphones. Sounds were recorded in mono with a sampling rate of 16 kHz and a bit depth of 16 bit. A band-pass filter is applied to remove information above and below the contact microphone's supported frequencies. For training, we split the data into $t = \{2s, 5s\}$ long audio samples with no overlap. These values are at the lower end of how long a human expert listens using a sounding stick. Samples are then preprocessed (Algorithm 1, Line 7) by either computing its mel-spectrogram or extracting eight

spectral features (chromagram, spectral centroid, spectral bandwidth, spectral contrast, spectral roll off, spectral flatness, zero-crossing rate and the root-mean-square value) which we have identified to be good descriptors of a leak during early stages of research. Each feature-vector is standardized by subtracting the mean and dividing by the standard-deviation of the individual features. Figure 3 provides more insights into the characteristics of the dataset. To evaluate the ability of our approach to differentiate between leak and no-leak, we use the following two datasets:

Leak in close proximity: To measure the ability to detect leaks in close proximity to a contact microphone, we select five consecutive days during which a leak was present in close proximity to contact microphone 1. For each day, we use the recordings from contact microphone 1 and one other contact microphone. This results in a balanced evaluation dataset with an equal number of leak and no-leak recordings.

Leak in the distance (synthetic): This setting measures how well a leak can be detected when it is farther away from a contact microphone. As we were only able to obtain recordings from a leakage near a single contact microphone, we mixed normal recordings with leak sounds having a high Signal-to-Noise Ratio of +24dB. Note that here noise stands for the leak sounds. Doing so yields synthetically generated recordings that resemble the characteristics of a leakage in the distance (Section 4). Synthetically creating anomalous recordings is a common approach when anomalous data is scarce (Duman et al., 2019; Purohit et al., 2019; Koizumi et al., 2019; Socoró et al., 2015; Stowell et al., 2015; Nakajima et al., 2016). We select 96 hours of no-leak recordings from contact microphones two and three. 48 hours of these recordings were mixed with randomly sampled leak sounds taken from a time-span between 0a.m. - 4a.m. This time-span was chosen as it yields pure leak sounds with very little noise.

5.2 Anomaly Detection Models

To compute anomaly scores for each individual sample (Algorithm 1, Line 8) we use various density estimation, ensemble models and deep neural networks. Models can be further subdivided according to the input they receive.

Mel-spectrogram Input A mel-spectrogram is a logarithmically scaled spectrogram to better align

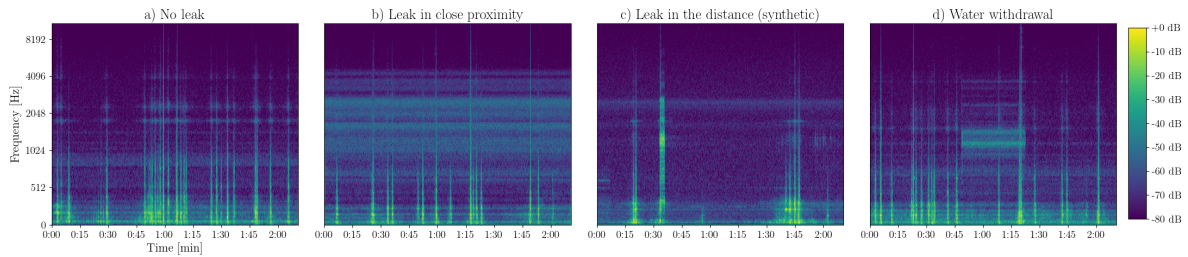


Figure 3: Four Mel-spectrograms depicting *a)* normal operation, *b)* a leak in close proximity, *c)* a synthetically generated distant leak and *d)* water withdrawal. Spikes are caused by cars driving over the hydrant cover above the contact microphones. However, other recordings may also contain footsteps, animal noises or interfering noises due to a nearby transformer house. A leak is characterized by high energy in the upper frequencies. This pattern becomes less dominant as the distance to the leak increases and vanishes after $\approx 600m$. The leak shown in *b)* has a throughput of $\approx 300 \frac{ml}{s}$.

Table 1: Average AUCs with standard deviations (over 5 seeds) for different settings of \mathcal{F} , h and t where $\phi = \text{median}$, $m = 20$, $h = 30\text{min}$ and $m = 40$, $h = 60\text{min}$.

Decision horizon h	Leak in close proximity				Leak in the distance (synthetic)			
	30min		60min		30min		60min	
Sample length t	2s	5s	2s	5s	2s	5s	2s	5s
GMM	74.8 \pm 2.5	88.0 \pm 1.3	74.6 \pm 2.1	87.6 \pm 1.6	64.0 \pm 5.5	68.7 \pm 0.0	68.4 \pm 1.0	70.0 \pm 1.2
B-GMM	78.7 \pm 3.7	88.1 \pm 2.4	78.8 \pm 4.0	87.7 \pm 2.6	64.0 \pm 5.1	70.5 \pm 1.8	69.3 \pm 1.2	72.5 \pm 2.9
IF	98.6 \pm 0.0	98.8 \pm 0.0	98.8 \pm 0.0	100 \pm 0.0	41.4 \pm 0.0	42.5 \pm 1.8	41.0 \pm 1.5	42.3 \pm 2.3
RealNVP	98.6 \pm 2.0	98.0 \pm 3.6	99.0 \pm 1.3	98.1 \pm 3.7	75.2 \pm 2.7	76.1 \pm 2.5	77.1 \pm 2.8	78.3 \pm 3.1
DCAE	98.2 \pm 0.0	98.9 \pm 0.0	99.8 \pm 0.0	100 \pm 0.0	75.1 \pm 1.5	73.4 \pm 5.0	76.1 \pm 2.1	76.0 \pm 3.3
AAE	98.9 \pm 0.0	99.0 \pm 0.0	99.8 \pm 0.0	99.8 \pm 0.0	75.0 \pm 4.4	69.9 \pm 3.2	77.0 \pm 5.2	71.6 \pm 2.4
AVB	98.1 \pm 0.5	99.5 \pm 0.1	99.6 \pm 0.5	100 \pm 0.0	76.9 \pm 3.4	75.5 \pm 2.7	78.9 \pm 3.7	77.5 \pm 2.8

with how humans perceive sound. We compute the mel-septograms with 64 mels, fft window = 2048 frames, hop length = 512 frames and normalize them to lie in the range $[0, 1]$. We also experimented with other settings but have found all methods to be robust against these parameters. The following deep neural networks are trained: *i)* *Deep Convolutional Auto Encoder* (DCAE) A neural network that compresses the input into a low dimensional representation and then reconstructs the input from this representation. We use $[4, 16, 32]$ convolution filters with 2×2 max-pooling in-between each layer with ReLU (Agarap, 2018) as activation function. We train for 100 epochs with a batch size of 128, a L2 weight penalty of 10^{-6} and optimize the AE using ADAM (Kingma and Ba, 2014) with a learning rate of 0.0001. For reconstruction, the inverse operations (deconvolution and up sampling) are applied in reverse order. *ii)* *Adversarial Auto Encoder* (AAE) (Makhzani et al., 2015) Adversarially trained DCAE such that the latent space spanned by the bottleneck features matches the prior distribution $\mathcal{N}(0, I)$. *iii)* *Adversarial Variational Bayes* (Mescheder et al., 2017) Adversarially trained variational DCAE.

Feature-Vector Input Here we extract eight spectral features (see Section 5) for each sample. The resulting feature vectors are used to train *i)* *Gaussian Mixture Model* (GMM) A density estimation algorithm that models the underlying probability distribution as a mixture of Gaussians. Parameters are estimated using expectation-maximization. We use 16 mixture components with diagonal covariance matrices. *ii)* *Bayesian Gaussian Mixture Model* (B-GMM) In contrast to a GMM, this model is trained using variational inference. We use the same parameters as for the GMM. *iii)* *RealNVP* (Dinh et al., 2017) A sequence of invertible transformations modeled by a neural network that can directly compute the probability density of the data. The approach is based on normalizing flows. We use 3 coupling layers, a hidden dimension of 150, a batch size of 768 and assume a normal distribution with zero mean and unit variance as base distribution. All of the methods above use the log-probability of a sample as normality score. *iv)* *Isolation Forest* (IF) (Liu et al., 2008) Recursively partitions the feature space. The number of splits needed to isolate a data point is used

as normality score. We use 120 base estimators.

Model performance is measured with the *Area Under the Receiver Operating Characteristics* (AUC) which quantifies how well a model can distinguish between leak and no-leak across all classification thresholds. The AUC is the standard metric to evaluate anomaly detection models across many domains (Aggarwal, 2015; Chalapathy and Chawla, 2019) as it yields a complete sensitivity/specificity report. The evaluation setup follows (Ruff et al., 2018).

5.3 Choosing the Model

The most important aspect of our approach is to choose a suitable score function \mathcal{F}_ϕ . The datasets presented in Section 5 are split into consecutive $h = 30\text{min}$ and $h = 60\text{min}$ long recordings. On each of these recordings, we run Algorithm 1 independently to obtain a single anomaly score. Here we chose the median as aggregation function ϕ due to its robustness against outliers¹ and evaluate across all models from Section 5.2 with $t = 2$ and $t = 5$. We set $m = 20$ and $m = 40$ for $h = 30\text{min}$ and $h = 60\text{min}$, respectively. Model parameters were determined using a small development set.

Results are depicted in Table 1. In the case of *Leak in close proximity* the performance of GMM and B-GMM is significantly worse compared to all other models. Interestingly, AUC-scores for GMM and B-GMM increase by approximately 12% when $t = 5$. This finding carries over the second setting as well. When $h = 60$ and $t = 5$ IF, DCAE and AVB reach perfect scores. Generally, the setting can be considered trivial for IF, RealNVP, DCAE, AVB and AAE. Note that in case of the AAE and AVB we also tried using the log-probability of the latent representation but the reconstruction error turned out to yield better results.

Results for *Leak in the distance (synthetic)* paint a different picture. In this setting, the differences between inlier and outlier are more subtle and therefore considerably harder to detect. IF fails completely on this task due to the reduced distance between inlier and outlier in feature space. The number of splits is the same for almost all samples and mostly depends on the random splitting points. Moreover, we observe general superiority of the neural network (NN) based methods RealNVP, DCAE, AVB and AAE indicating that NNs better reveal the more subtle differences. On

¹The median showed the best results compared to other aggregation functions like the mean. Using only the most normal sample (min-pooling) leads to a comparable, but worse performance.

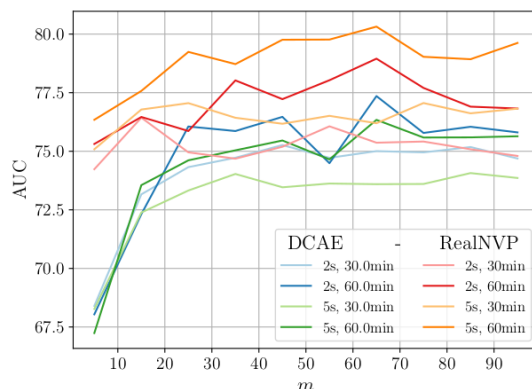


Figure 4: Performance comparison for $m = \{5, 15, 25, \dots, 105\}$ on *Leak in the distance (synthetic)*. Each value is the average AUC over 5 seeds.

2s, Mel-spectrogram based AVB performs best and on 5s RealNVP outperforms all other methods. We observed that auto encoders work best with a small bottleneck as this limits their ability to generalize over leak patterns based on water withdrawal. Moreover, we can verify that the extracted feature set is indeed a good leak indicator as it shows strong performance when used in conjunction with NN based RealNVP.

5.4 Choosing the Number of Samples

In this experiment, we evaluate upon the influence of the number of samples on the model performance. In figure 4, we vary the number of samples m from 5 to 105 in steps of 10 samples. We evaluate across all combinations of decision horizon $h \in \{30\text{min}, 60\text{min}\}$ and sample length $t \in \{2\text{s}, 5\text{s}\}$ on *Leak in the distance (synthetic)* with $\phi = \text{median}$. For better clarity, we only show results for RealNVP and DCAE.

In Figure 4, we observe that using less than 15 samples yields significantly worse performance. Results stabilize thereafter and peak performance is achieved at $m = 65$ for most settings. We conclude that increasing the number of samples has a positive effect on the performance because it makes the decision less dependent on individual samples. More samples better represent the underlying distribution as a leak is characterized by a constantly present acoustic pattern. In contrast to a streaming approach, only a fraction of all possible measurements has to be considered as we did not observe a substantial increase in performance by considering even more samples.

6 Conclusion

In this work, we presented a general procedure for leak detection in water networks that satisfies real-world constraints and provided a thorough evaluation of different parameter settings. While a leak in close proximity to a contact microphone is trivial for most scoring functions, neural network based approaches yielded superior results with respect to the detection of a (synthetic) leak in the distance. Additionally, we found that it is not necessary to constantly monitor the system. It suffices to consider a fraction of the recordings during a predefined decision horizon.

7 Future Work

Future work might investigate further upon different scoring functions, e.g. by taking the sequential nature of the recordings into account. Other avenues worth exploring are more sophisticated sampling and aggregation strategies. The extension of our approach to leak localization (e.g. via trilateration) represents the next logical step. Moreover, instead of training a single model on data from all contact-microphones, one might train separate models. Another possibility would be to use weight sharing and condition (Huang and Belongie, 2017) the model on the contact-microphone ID or on features of their surrounding. Another important aspect that still remains to be investigated, is how to update the model when new data (possibly collected in another area) arrives (Koizumi et al., 2020).

Acknowledgments

This work is part of the research project *ErLoWa* which was carried out in cooperation with Stadtwerke München GmbH.

REFERENCES

- Adedeji, K. B., Hamam, Y., Abe, B. T., and Abu-Mahfouz, A. M. (2017). Towards achieving a reliable leakage detection and localization algorithm for application in water piping networks: An overview. *IEEE Access*, 5:20272–20285.
- Agarap, A. F. (2018). Deep learning using rectified linear units (relu). *arXiv preprint arXiv:1803.08375*.
- Aggarwal, C. C. (2015). Outlier analysis. In *Data mining*, pages 237–263. Springer.
- Chalapathy, R. and Chawla, S. (2019). Deep learning for anomaly detection: A survey. *arXiv preprint arXiv:1901.03407*.
- Chan, T., Chin, C. S., and Zhong, X. (2018). Review of current technologies and proposed intelligent methodologies for water distributed network leakage detection. *IEEE Access*, 6:78846–78867.
- Chuang, W.-Y., Tsai, Y.-L., and Wang, L.-H. (2019). Leak detection in water distribution pipes based on cnn with mel frequency cepstral coefficients. In *Proceedings of the 2019 3rd International Conference on Innovation in Artificial Intelligence*, pages 83–86.
- Cody, R., Narasimhan, S., and Tolson, B. (2017). One Class SVM – Leak Detection in Water Distribution Systems’.
- Cody, R. A., Tolson, B. A., and Orchard, J. (2020). Detecting leaks in water distribution pipes using a deep autoencoder and hydroacoustic spectrograms. *Journal of Computing in Civil Engineering*, 34(2).
- Dinh, L., Sohl-Dickstein, J., and Bengio, S. (2017). Density estimation using real NVP. In *5th International Conference on Learning Representations, ICLR 2017*.
- Duman, T. B., Bayram, B., and İnce, G. (2019). Acoustic anomaly detection using convolutional autoencoders in industrial processes. In *International Workshop on Soft Computing Models in Industrial and Environmental Applications*, pages 432–442. Springer.
- El-Zahab, S. and Zayed, T. (2019). Leak detection in water distribution networks: an introductory overview. *Smart Water*, 4(1):5.
- Gao, Y., Brennan, M. J., Liu, Y., Almeida, F. C., and Joseph, P. F. (2017). Improving the shape of the cross-correlation function for leak detection in a plastic water distribution pipe using acoustic signals. *Applied Acoustics*, 127:24–33.
- Hayashi, T., Komatsu, T., Kondo, R., Toda, T., and Takeda, K. (2018). Anomalous sound event detection based on wavenet. In *2018 26th European Signal Processing Conference (EUSIPCO)*, pages 2494–2498. IEEE.
- Huang, X. and Belongie, S. (2017). Arbitrary style transfer in real-time with adaptive instance normalization. In *Proceedings of the IEEE International Conference on Computer Vision*, pages 1501–1510.
- Kang, J., Park, Y.-J., Lee, J., Wang, S.-H., and Eom, D.-S. (2017). Novel leakage detection by ensemble cnn-svm and graph-based localization in water distribution systems. *IEEE Transactions on Industrial Electronics*, 65(5):4279–4289.
- Kingma, D. P. and Ba, J. (2014). Adam: A method for stochastic optimization. *arXiv preprint arXiv:1412.6980*.
- Koizumi, Y., Saito, S., Uematsu, H., and Harada, N. (2017). Optimizing acoustic feature extractor for anomalous sound detection based on neyman-pearson lemma. In *2017 25th European Signal Processing Conference (EUSIPCO)*, pages 698–702. IEEE.
- Koizumi, Y., Saito, S., Uematsu, H., Harada, N., and Imoto, K. (2019). Toyadmos: A dataset of miniature-machine operating sounds for anomalous sound detection. In *2019 IEEE Workshop on Applications of*

- Signal Processing to Audio and Acoustics (WASPAA)*, pages 313–317. IEEE.
- Koizumi, Y., Yasuda, M., Murata, S., Saito, S., Uematsu, H., and Harada, N. (2020). Spidernet: Attention network for one-shot anomaly detection in sounds. In *ICASSP 2020-2020 IEEE International Conference on Acoustics, Speech and Signal Processing (ICASSP)*, pages 281–285. IEEE.
- Li, Y., Li, X., Zhang, Y., Liu, M., and Wang, W. (2018). Anomalous sound detection using deep audio representation and a blstm network for audio surveillance of roads. *IEEE Access*, 6:58043–58055.
- Liu, F. T., Ting, K. M., and Zhou, Z.-H. (2008). Isolation forest. In *2008 Eighth IEEE International Conference on Data Mining*, pages 413–422. IEEE.
- Makhzani, A., Shlens, J., Jaitly, N., Goodfellow, I., and Frey, B. (2015). Adversarial autoencoders.
- Marchi, E., Vesperini, F., Eyben, F., Squartini, S., and Schuller, B. (2015). A novel approach for automatic acoustic novelty detection using a denoising autoencoder with bidirectional lstm neural networks. In *2015 IEEE International Conference on Acoustics, Speech and Signal Processing (ICASSP)*, pages 1996–2000. IEEE.
- Meire, M. and Karsmakers, P. (2019). Comparison of deep autoencoder architectures for real-time acoustic based anomaly detection in assets. In *2019 10th IEEE International Conference on Intelligent Data Acquisition and Advanced Computing Systems: Technology and Applications (IDAACS)*, volume 2, pages 786–790. IEEE.
- Mescheder, L., Nowozin, S., and Geiger, A. (2017). Adversarial variational bayes: Unifying variational autoencoders and generative adversarial networks. In *Proceedings of the 34th International Conference on Machine Learning-Volume 70*, pages 2391–2400. JMLR.org.
- Muggeleton, J. and Brennan, M. (2004). Leak noise propagation and attenuation in submerged plastic water pipes. *Journal of Sound and Vibration*, 278(3):527–537.
- Müller, R., Ritz, F., Illium, S., and Linnhoff-Popien, C. (2020). Acoustic anomaly detection for machine sounds based on image transfer learning. *arXiv preprint arXiv:2006.03429*.
- Nakajima, Y., Naito, T., Sunago, N., Ohshima, T., and Ono, N. (2016). Dnn-based environmental sound recognition with real-recorded and artificially-mixed training data. In *INTER-NOISE and NOISE-CON Congress and Conference Proceedings*, volume 253, pages 1832–1841. Institute of Noise Control Engineering.
- Nguyen, D., Kirsebom, O. S., Frazão, F., Fablet, R., and Matwin, S. (2019). Recurrent neural networks with stochastic layers for acoustic novelty detection. In *ICASSP 2019-2019 IEEE International Conference on Acoustics, Speech and Signal Processing (ICASSP)*, pages 765–769. IEEE.
- Ni, Q.-Q. and Iwamoto, M. (2002). Wavelet transform of acoustic emission signals in failure of model composites. *Engineering Fracture Mechanics*, 69(6):717–728.
- Oord, A. v. d., Dieleman, S., Zen, H., Simonyan, K., Vinyals, O., Graves, A., Kalchbrenner, N., Senior, A., and Kavukcuoglu, K. (2016). Wavenet: A generative model for raw audio. *arXiv preprint arXiv:1609.03499*.
- Purohit, H., Tanabe, R., Ichige, K., Endo, T., Nikaido, Y., Suefusa, K., and Kawaguchi, Y. (2019). Mimmii dataset: Sound dataset for malfunctioning industrial machine investigation and inspection. In *Acoustic Scenes and Events 2019 Workshop (DCASE2019)*, page 209.
- Ruff, L., Vandermeulen, R., Goernitz, N., Deecke, L., Siddiqui, S. A., Binder, A., Müller, E., and Kloft, M. (2018). Deep one-class classification. In *International Conference on Machine Learning*, pages 4393–4402.
- Rushe, E. and Namee, B. M. (2019). Anomaly detection in raw audio using deep autoregressive networks. In *ICASSP 2019 - 2019 IEEE International Conference on Acoustics, Speech and Signal Processing (ICASSP)*, pages 3597–3601.
- Socoró, J. C., Ribera, G., Sevillano, X., and Alías, F. (2015). Development of an anomalous noise event detection algorithm for dynamic road traffic noise mapping. In *Proceedings of the 22nd International Congress on Sound and Vibration (ICSV22), Florence, Italy*, pages 12–16.
- Stoianov, I., Nachman, L., Madden, S., Tokmouline, T., and Csail, M. (2007). Pipenet: A wireless sensor network for pipeline monitoring. In *2007 6th International Symposium on Information Processing in Sensor Networks*, pages 264–273.
- Stowell, D., Giannoulis, D., Benetos, E., Lagrange, M., and Plumbley, M. D. (2015). Detection and classification of acoustic scenes and events. *IEEE Transactions on Multimedia*, 17(10):1733–1746.
- Suefusa, K., Nishida, T., Purohit, H., Tanabe, R., Endo, T., and Kawaguchi, Y. (2020). Anomalous sound detection based on interpolation deep neural network. In *ICASSP 2020-2020 IEEE International Conference on Acoustics, Speech and Signal Processing (ICASSP)*, pages 271–275. IEEE.
- SWM, P. (2018). Die swm vernetzen münchen: Lora-netz am start für das internet der dinge. <https://www.swm.de/dam/swm/pressemitteilungen/2018/06/20180604-swm-bauen-lora-netz-auf.pdf>.
- Ting, L., Tey, J., Tan, A., King, Y., and Faizd, A. (2019). Improvement of acoustic water leak detection based on dual tree complex wavelet transform-correlation method. In *IOP Conference Series: Earth and Environmental Science*, volume 268. IOP Publishing.
- WaterUK (2020). Leaking pipes. <https://discoverwater.co.uk/leaking-pipes>. Accessed: 2020-01-20.